Front. Chem. Sci. Eng. 2021, 15(5): 1088–1098
https://doi.org/10.1007/s11705-020-1969-y

RESEARCH ARTICLE

Synthesis of boron modified $CoMo/Al_2O_3$ catalyst under different heating methods and its gasoline hydrodesulfurization performance

Hui Shang (✉), Chong Guo*, Pengfei Ye*, Wenhui Zhang

State Key Laboratory of Heavy Oil Processing, China University of Petroleum (Beijing), Beijing 102249, China

Abstract Catalytic hydrodesulfurization (HDS) technique is widely used for clean gasoline production. However, traditional HDS catalyst ($CoMo/\gamma$-Al_2O_3) exhibits high hydrogenation performance of olefins (HYDO), resulting in the loss of gasoline octane number. To achieve high HDS/HYDO ratio, the key issue is to reduce the interaction between active metals and the support, therefore, in this research, the modified $CoMo/\gamma$-Al_2O_3 catalysts with various boron amounts were investigated under traditional or microwave heating. The effects of preparing methods as well as boron amounts on the active phase, acidic properties and HDS catalytic activities were examined. Results show that the modification, especially under microwave treatment, can significantly weaken the interaction between the active component and the support by enlarging the surface area and pore diameter, and reducing the acidity of the support. As a result, the stacking numbers of MoS_2 slabs were obviously improved by the modification and microwave treatment, contributing to higher edge/rim ratio, and resulting in higher HDS performance and selectivity to olefin.

Keywords CoMo catalyst, boron modification, surface acidity, microwave heating, selective hydrodesulfurization

1 Introduction

Today, with the new strict environmental regulations, the maximum sulfur content allowed in transportation fuels has been reduced, in many countries, to very low levels (less than 10 $mg \cdot L^{-1}$) [1,2]. In China, fluid catalytic cracking (FCC) gasoline is the major sulfur contributor to commercial gasoline. Hydrodesulfurization (HDS) is an effective technology for clean gasoline production [3]. Hydrotreating catalysts with Co(Ni)-Mo mixed sulfide on an acidic carrier such as γ-alumina are widely used in the HDS processes. However, traditional HDS catalyst exhibits high activities for both HDS and hydrogenation of olefins, and the latter will cause a serious loss of gasoline octane number [4]. Hence, the design and preparation of highly active catalysts with lower hydrogenation activity are highly desirable.

In recent years, considerable efforts have been made to develop the $CoMo/Al_2O_3$ catalyst to improve the HDS activity and selectivity. It has been well accepted that the morphology and catalytic activities of the HDS catalyst mainly depend on the crystallographic structure and surface properties of the alumina support [5]. The Co-Mo-S model, proposed by Topsøe et al. [6–8], where Co located on the edge sites of highly dispersed MoS_2 crystallites, has been accepted as the catalytically active phase in CoMo sulfide catalysts. Based on their intrinsic catalytic activities, there are two types of Co-Mo-S phases. It is believed that the Co-Mo-S I is associated with highly dispersed single-layer MoS_2 particles, maintaining strong interactions with the support by forming Mo-O-Al bond; whereas Co-Mo-S II phase is related to MoS_2 particles mainly stacked and not linked to the support, showing higher intrinsic HDS activities [9]. It is known that HDS performance depends on the physicochemical properties of the support. The interaction between the alumina and the active metal oxide precursor is a crucial factor in determining the metal dispersibility. A strong interaction may result in poor sulfidation of Mo species, as well as partial loss of the promoter to the alumina matrix by forming an inactive spinel structure during the hydrotreating reaction [10]. In order to control the surface properties of the support and the dispersibility and reactivity of the active phases, the support is often modified.

Boron modification of the hydrotreating catalysts has unraveled that the application of boron provokes changes

Received April 20, 2020; accepted June 8, 2020

E-mail: huishang@cup.edu.cn

*These authors contributed equally to this work.

in structural characteristics, the acidic properties of the supports and catalysts, the morphology of the active components, and the catalytic activity in HDS reactions [11–17]. Peil et al. [1] confirmed that with the incorporation of boron to the catalyst, the acidity of the carrier was adjusted, resulting in higher activities of $CoMo/Al_2O_3$ and $NiMo/Al_2O_3$ catalysts for HDS reactions. Similarly, boron introduction can regulate Brønsted acidity of the supports and modify the electronic properties of the sulfide sites [10,19]. Changing acidity may associate with different interactions of boron with alumina. Houalla and Delmon [20] proposed that the alumina acidity increased due to the boron addition through the formation of Al-O-B-O-Al bonds. However, most researches highlighted that the addition of boron decreased the chemical interaction between the supported metal and alumina. Usman et al. [16] concluded that boron modification improved the catalyst's performance by weakening the interactions between molybdenum oxides and Al_2O_3 surface, thus leading to a shift of the types from a less active Co-Mo-S I to a more active Co-Mo-S II phases. The weakened interactions between Mo species and Al_2O_3 surface concomitantly resulted in a decrease in the dispersion of Mo species in $CoMo/Al_2O_3$ catalysts, in agreement with the results of Morishige and Akai [21]. Furthermore, Lewandowski and Sarbak [22,23] found that boron did not change the pore volumes significantly, while increased the pore diameters to 20, 25, 30 and 40 Å in comparison with the unmodified catalyst, resulting in better sulfidation of the supported metals. Moreover, the combination usage of boron with other additives, such as phosphorus [24,25] or fluorine [15], will intensify a positive boron influence.

Microwave heating technology has been employed to improve the desulfurization performance of liquid fuels due to its dedicated heating mechanism [26]. Furthermore, it has been revealed by several researches that the active components of the catalyst prepared by microwave were uniformly distributed, and the load amount was highly increased [27–29]. Researchers also embodied that the HDS catalysts prepared by microwave exhibited lower metal-support interaction (MSI), higher reaction performance [30,31]. However, the preparation of boron modified HDS catalyst under microwave conditions has not been reported. This paper systematically studied the application of microwave in catalyst preparation. Alumina decorated with B was used as a support for CoMo catalyst. Catalysts' characteristics and their HDS performance were investigated in detail.

2 Experimental

2.1 Supports preparation

The pseudo-boehmite was used as a precursor of the alumina carrier and calcined in a muffle furnace at 500 °C for 6 h to prepare γ-Al_2O_3 support, labeled as AlB-0. While AlB-x was denoted as the catalyst with B_2O_3 loading content of x%.

A series of B_2O_3/γ-Al_2O_3 modified supports were prepared by the incipient wetness impregnation method (adopting 35% excess solvent) and referred as AlB-0.5, AlB-1.0, and AlB-2.0, respectively. Boric acid (Aladdin, China) as a source of boron was dissolved in distilled water to prepare the impregnation solution, the solution was then added to the pre-weighed γ-alumina and dried at 80 °C and 120 °C for 2 h respectively, and underwent calcination at 500 °C for 6 h to obtain B_2O_3/γ-Al_2O_3 supports. Similarly, the boron-modified γ-Al_2O_3 containing 2.0% B_2O_3 under microwave irradiation was named as AlB-2.0(MW). Whereas when used microwave, the drying time was shortened to 1 h at the same temperatures, and the calcination at 500 °C was only for 2 h.

2.2 Catalysts preparation

The above boron-modified γ-Al_2O_3 supports were used to prepare CoMo catalysts by the incipient wetness impregnation method (adopting 35% excess solvent). Hexaammonium molybdate ($(NH_4)_6Mo_7O_{24}\cdot 4H_2O$, 1.8391 g, Aladdin, China) was dissolved in 28.53 g of ammonia ($NH_3\cdot H_2O$, 25 wt-%, Tianjin Fuchen Chemical Reagents Factory) at 50 °C. Cobalt nitrate ($Co(NO_3)_2\cdot 6H_2O$, 1.9402 g, Aladdin, China) was then slowly added to the above solution. After impregnation of the modified support with the mixture, the catalysts thermally treated at 500 °C in the atmosphere of air for 6 h and was then tableted and crushed to 40−60 mesh for use. All catalysts contained 15 wt-% MoO_3 and 5 wt-% CoO.

2.3 Catalyst characterization

N_2 adsorption-desorption isotherms were performed to measure the surface area and pore structure properties of the supports on an automated gas sorption instrument (Micromeritics TriStar 3020). The specific surface area was determined by the Brunauer-Emmett-Teller (BET) formula, and the pore size distribution was obtained via the Barrett-Joyner-Halenda method.

Scanning electron microscopic analysis (SEM, ZEISS GeminiSEM 300) was used to study the surface structures.

Acidic characterization of the oxidized supports was carried out on PerkinElmer Lambda 950 infrared spectrometer. The pyridine-Fourier transform infrared (py-FTIR) spectra of the catalysts were collected at 200 °C and 350 °C using a spectrophotometer, while 200 °C spectra were used to calculate the number of total acid sites, and the 350 °C counterpart were used to calculate the number of the strong acid sites. The acids amount can be calculated as follows:

$$C_B = \frac{1.88 \cdot A_B \cdot R^2}{m}, \quad (1)$$

$$C_{\mathrm{L}} = \frac{1.42 \cdot A_{\mathrm{L}} \cdot R^2}{m}, \quad (2)$$

where C_{B} and C_{L} represent the acid amounts of Bronsted (B) acid and Lewis (L) acid ($\mathrm{mmol \cdot g^{-1}}$), respectively. R is the radius (cm) of the tablet sample, and m is the sample mass (mg). A_{B} and A_{L} are the peak areas of the absorption peaks of Bronsted acid and Lewis acid, respectively.

Analysis of H_2 temperature-programmed reduction (H_2-TPR) was carried out on a ChemStar TPX (Anton Paar) with 0.1 g oxidized catalysts. The samples were first pretreated at 450 °C for 2 h under Ar stream and then cooled to room temperature. After that, the sample was heated to 1000 °C at a rate of 10 $\mathrm{°C \cdot min^{-1}}$ in H_2/Ar mixed gases (10 vol-% Ar) with a flow rate of 40 $\mathrm{mL \cdot min^{-1}}$. A thermal conductivity detector recorded the signals to obtain TPR curves.

High-resolution transmission electron microscopy (HRTEM) measurement for the sulfided catalysts was carried out on a Tecnai G^2 STWIN field emission transmission electron microscope (FEI F20, USA). The quantitative statistical analysis of the stacking layer number and the length of MoS_2 slabs have been applied based on at least 20 representation micrographs taken from different parts of the sample, about 400–600 slabs were counted for each catalyst. Combining the statistical results with the following formulas to calculate the average slab length ($\overline{L}$) and stacking number ($\overline{N}$). MoS_2 dispersion (D_{Mo}) is determined by the following equations:

$$\overline{L} = \frac{\sum_{i=1}^{n} x_i L_i}{\sum_{i=1}^{n} x_i}, \quad (3)$$

$$\overline{N} = \frac{\sum_{i=1}^{n} x_i N_i}{\sum_{i=1}^{n} x_i}, \quad (4)$$

where L_i and N_i are the length of MoS_2 slab and the number of stacking layers, respectively, and x_i is the number of slabs with the length of L_i.

$$D_{\mathrm{Mo}} = \frac{\mathrm{Mo_e} + \mathrm{Mo_c}}{\mathrm{Mo_T}} = \frac{\sum_{i=1}^{t} (6n_i - 6)}{\sum_{i=1}^{t} (3n_i^2 - 3n_i + 1)}, \quad (5)$$

where $\mathrm{Mo_e}$ and $\mathrm{Mo_c}$ are the numbers of Mo atoms at the edge and corner sites; $\mathrm{Mo_T}$ is the total number of Mo atoms; n_i is the number of Mo atoms along one side of a MoS_2 slab calculated by its length ($L = 3.2 \times (2n_i - 1)$ Å), and t is the total number of layers in the HRTEM micrographs

X-ray photoelectron spectroscopy (XPS) analysis of the sulfided catalysts was performed on a Thermo Fisher K-Alpha spectrometer (USA). Sulfurized catalysts are obtained under the same reaction conditions as the catalytic activity evaluation in the following section. The C1*s* peak (284.8 eV) was used as the reference for calibration. The relative contents of MoS_2, Mo^{5+}, Mo^{6+}, Co-Mo-S, Co_9S_8 and Co^{2+} species were obtained by using the XPSPEAK software.

2.4 Catalytic performance evaluation

The HDS performance was investigated in a continuous fixed-bed reactor loaded with 3.0 g catalyst. All fresh catalysts were presulfided with a mixture of H_2 and a stream containing 3 wt-% CS_2 in cyclohexane; presulfiding reactions were carried out in four steps at 150 °C 1 h, at 230 °C 1 h, at 280 °C 1 h and 320 °C 4 h respectively.

After pre-sulfidation, the HDS activity and selectivity to olefin were studied of FCC gasoline achieved from Yanshan Petrochemical Co., Ltd. (sulfur content: 510 $\mathrm{mg \cdot L^{-1}}$). The hydrotreating experiments were carried out under the following conditions: weight hourly space velocity = 2.0 $\mathrm{h^{-1}}$, P = 2 MPa, H_2/oil = 200 (vol/vol), and T = 220 °C–260 °C.

The activity and selectivity of the catalysts can be calculated based on Eqs. (6–8):

$$HDS\% = \frac{S_{\mathrm{f}} - S_{\mathrm{p}}}{S_{\mathrm{f}}} \times 100, \quad (6)$$

$$HYDO\% = \frac{O_{\mathrm{f}} - O_{\mathrm{p}}}{O_{\mathrm{f}}} \times 100, \quad (7)$$

$$\frac{HDS}{HYDO} = \frac{\ln(1 - HDS\%)}{\ln(1 - HYDO\%)}, \quad (8)$$

where S_{f} and S_{p} are the mass fractions of sulfides in the feedstock and products, which were analyzed using an Agilent 7890A sulfur chromatography. O_{f} and O_{p} are the mass fractions of olefins in the feedstock and products, which are determined by gas chromatography.

3 Results and discussion

3.1 Structure characterization

The N_2 adsorption-desorption isotherms of the supports were analyzed and shown in Fig. 1. The textural and structural characterization results are listed in Table 1. The adsorption-desorption isotherms of the AlB-0, AlB-2.0 and AlB-2.0(MW) exhibit obvious hysteresis loop, which

belong to typical type IV adsorption isotherm, indicating of the mesoporous structure. As shown in Table 1, the surface areas of modified alumina under conventional treatment show an apparent decrease in the textural characteristics (for example, surface areas, volumes and average pore sizes), which should be caused by the impregnation method prepared for the modified supports. However, the textural characteristics have been found significantly improved by microwave heating.

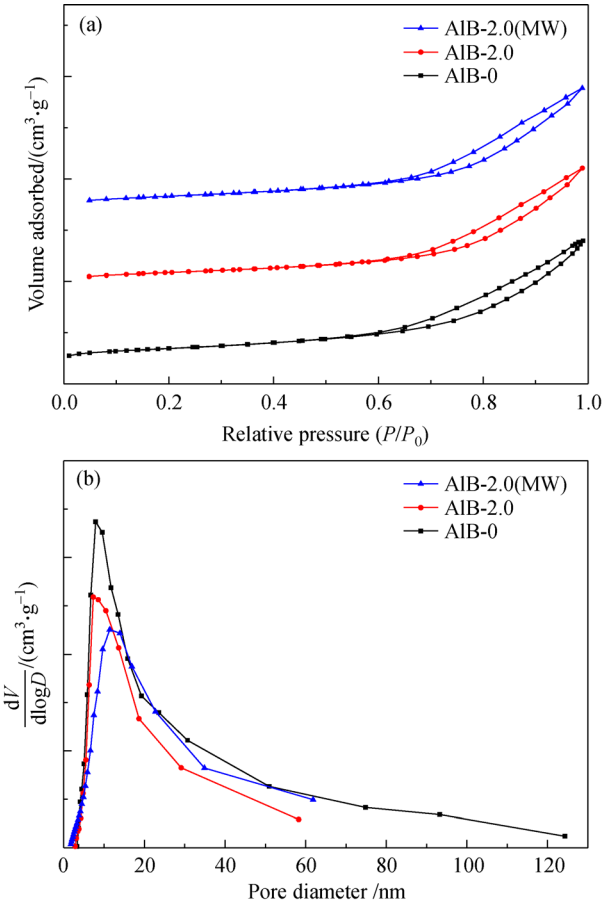

Fig. 1 (a) N_2 adsorption-desorption isotherms and (b) pore size distribution curves of prepared supports: AlB-0, AlB-2.0 and AlB-2.0(MW).

Table 1 Textural properties of the prepared supports

Samples	S_{BET}/($m^2 \cdot g^{-1}$)	V/($cm^3 \cdot g^{-1}$)	D_{BIH}/nm
AlB-0	301	0.9400	8.1
AlB-2.0	269	0.9046	7.3
AlB-2.0(MW)	292	0.9406	11.7

The increase of the surface area of microwave prepared supports is thought due to the rapid and selective heating of dipole molecules under microwaves, which would cause rapid dehydroxylation and the formation of more clean and open pore structures as verified through the SEM images (as shown in Fig. 2). From the images, after the introduction of boron to the alumina, there is no obvious difference between AlB-0 and AlB-2.0. However, a significant distinction can be found between AlB-2.0 and AlB-2.0(MW), indicating that microwave electrified has a major effect on the preparation of alumina supports. In the conventional method, the support is heated by convective heat transfer from the high-temperature area and by conduction from the surface to the core. The temperature on the surface is higher due to the poor thermal conductivity of alumina support, making the process of dihydroxylation difficult. However, the principle of microwave heating is based on the interaction between the electromagnetic field and the polar molecules, so that the energy transfer is not governed by conduction or convection as in conventional heating [32]. Thus, the temperature inside the support is higher than its surface due to the inside heat cannot escape in time, resulting in rapid dihydroxylation process. The inner paths of the pores were mainly formed during hydroxyl removal.

3.2 Py-FTIR characterization of supports

Py-FTIR spectroscopy was employed to determine the strength and types of acid sites of the supports (Fig. 3). The total number of acid sites obtained based on the py-FTIR spectra at 200 °C, and the 350 °C counterpart were used to calculate the number of strong acid sites. It is obvious that four peaks at 1450, 1488, 1576 and 1617 cm^{-1} in the range of 1400–1700 cm^{-1} are observed, which can be ascribed to Lewis acid sites according to the literature [33–35]. The adsorption peak at 1540 cm^{-1} which is considered as Brønsted acid site was not detected. It can be seen that the boric acid-modified supports result in a decrease in the amount of total acid sites from 102.6 to 71.5 $\mu mol \cdot g^{-1}$ and medium and strong acid sites decrease from 55.8 to 47.7 $\mu mol \cdot g^{-1}$. Adopting to microwave heating instead of traditional heating to prepare binary composite supports, the amount of total acid sites increased slightly to 83.9 $\mu mol \cdot g^{-1}$, while the amount of strong acid on the surface of boron-modified alumina was further reduced to 28.8 $\mu mol \cdot g^{-1}$. These results are attributed to the interaction between boron acid and hydroxyl groups, which may lead to the consumption of more hydroxyl groups [36]. The introduction of microwave may promote this reaction.

3.3 H_2 temperature-programmed reduction

In order to investigate the interaction between the active components and support, the catalyst was characterized through H_2-TPR. It can be seen from Fig. 4 that the prepared catalysts exhibit two extinctive peaks in the ranges of 350 °C–550 °C and 700 °C–950 °C. The

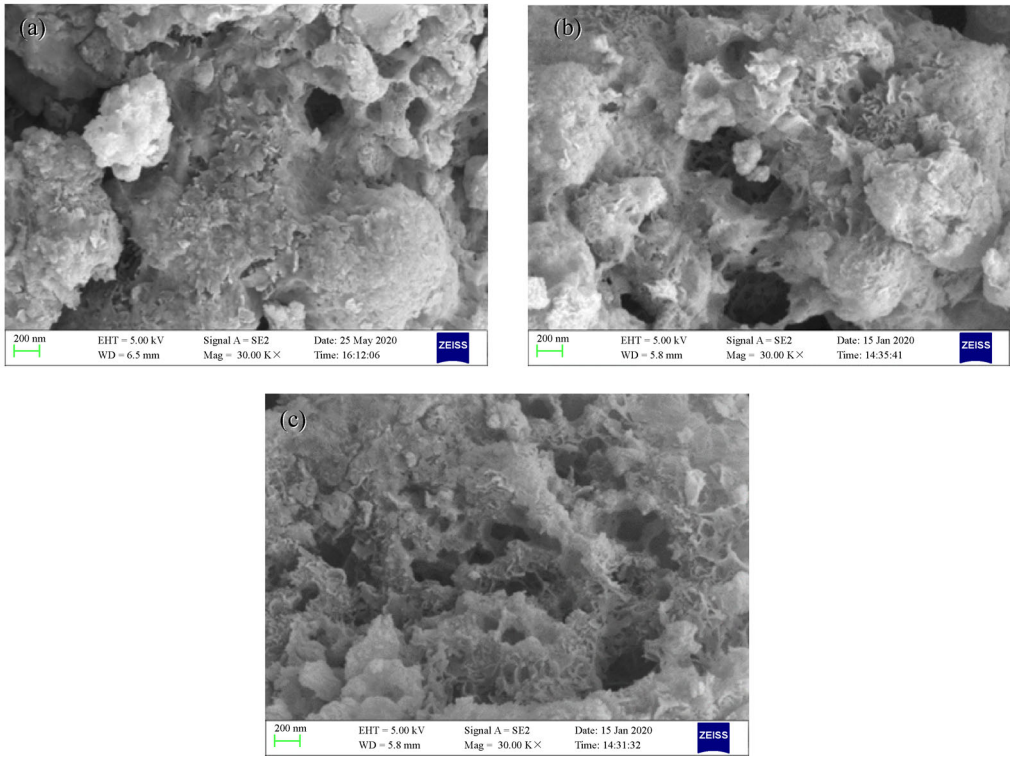

Fig. 2 SEM images of (a) AlB-0, (b) AlB-2.0 and (c) AlB-2.0(MW).

low-temperature peak originates from the reduction of Mo (Mo^{6+} to Mo^{4+}) of the octahedrally polymetric hexa-coordinated Mo species, indicating a weaker MSI, which favors the formation of Co-Mo-S II type phase; the high-temperature peak corresponds to the deep reduction (Mo^{4+} to Mo^{0}) of the tetrahedral coordinated monomeric Mo species ($[Al_2(MoO_4)_3]$) and maintains a strong MSI [37]. Apparently, the addition of boron strongly shifted both peaks to the left, which manifests that boron addition could weaken the strength of metal-support, making the metal oxides easier for reduction. Furthermore, the area of the low-temperature reduction peak was significantly improved, suggesting that boron not only weakened the mutual interaction between the active component and the support, but also increased the number of octahedral hexa-coordinated Mo species. The decrease in the reduction temperature and the increase of the low-temperature peak area further suggest that boron modification can effectively reduce the MSI and is beneficial to the formation of the active Co-Mo-S II active phase in the subsequent sulfidation process. The results are consistent with the above py-FTIR analysis. The reason is mainly thought to be due to the formation of Al-O-B-O-Al after boron insertion, which would reduce hydroxyl groups, weaken the MSI [20].

According to the reports in the literature, microwave can alter the interaction between the active component and the support [31]. Therefore, the 2% boron modified catalyst prepared by conventional and microwave heating methods were characterized by H_2-TPR. From Fig. 4, the reduction peak of AlB-2.0(MW) has a further shift to the left compared to that of AlB-2.0. It is worth noting that the peak area of low-temperature reduction peak of AlB-2.0 (MW) becomes larger, highlighting that microwave-assisted preparation of AlB-2.0(MW) support can induce a larger number of octahedral hexa-coordinated Mo species with weaker interaction with the support, forming more highly active Co-Mo-S II phases after sulfuration. In addition, AlB-2.0(MW) exhibits another peak at 525 °C, which may be the reduction peak of β-$CoMoO_4$, which is thought of a good precursor to form Co-Mo-S active phase since the interaction between β-$CoMoO_4$ and alumina support is weak and thus prevents the loss of Co to inactive species such as $CoAl_2O_4$ and Co_3O_4 [38–40].

3.4 HRTEM of sulfide catalysts

The specific distribution of active components over alumina surface after boron modification was investigated. HRTEM characterization was carried out on AlB-0, AlB-2.0, AlB-2.0(MW) catalysts respectively to study the effect of microwave heating on the morphology of active components. The typical morphology of MoS_2 slabs is displayed in Fig. 5, wherein the black linear stripes belong to MoS_2 slabs. The distribution of slab lengths and stacking layer numbers of MoS_2 crystallites are presented in Fig. 6.

Suitable higher stacking layer numbers of MoS_2

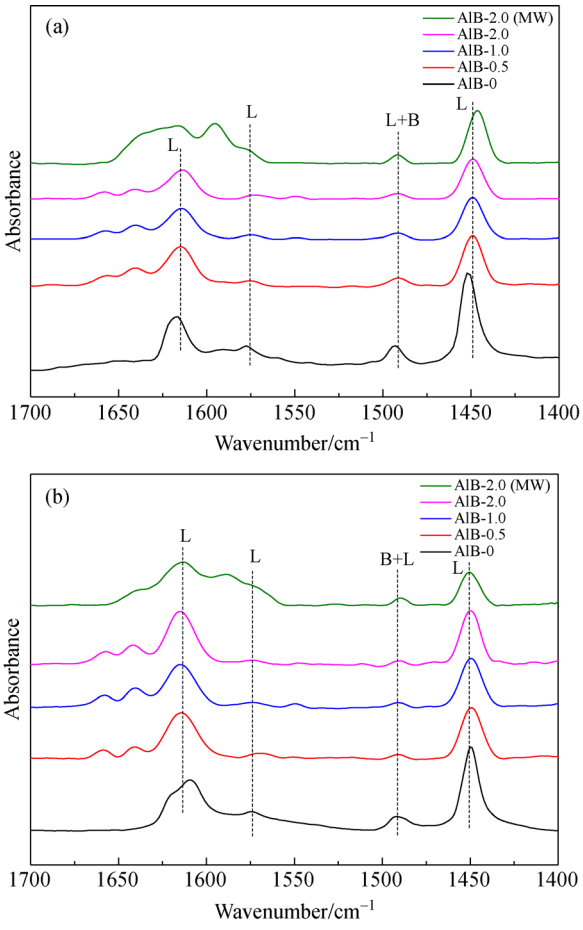

Fig. 3 Py-FTIR spectra of different boron contents over the modified supports at (a) 200 °C and (b) 350 °C. L represents Lewis acid and B for Brønsted acid.

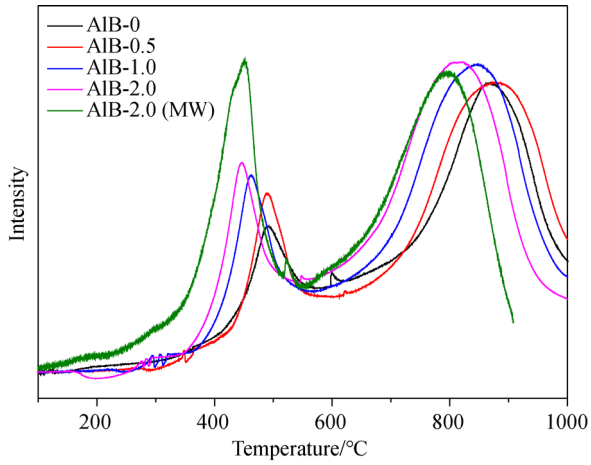

Fig. 4 H_2-TPR curves of different boron contents over the modified catalysts.

crystallites facilitate the formation of more Co-Mo-S II active phases [4]. MoS_2 phases over AlB-0 catalyst are mainly distributed in monolayer, which processes more Mo-O-Al bonds resulting in strong MSI, and more Co-Mo-S I phases [39]. However, AlB-2.0 catalyst contains a higher degree of stacking slabs, with the proportion of monolayer structure decreasing sharply from 65% to about 20%, while the proportion of two-layer and three-layer structures climbing to 35% and 15% respectively, and that of the four-layer structure from the original 1% to 13%. It confirms that boron modification can effectively weaken the MSI, thereby increase the number of stacking layers of the active phase and the desulfurization active sites.

The HRTEM results are consistent with those from H_2-TPR analysis. Compared with AlB-2.0, the AlB-2.0(MW) catalyst prepared by microwave heating exhibits a weaker MSI by further reducing the proportion of the monolayer and two-layer structures from 20% to about 10%, and 34% to 30%, respectively, but boosting those of the three- and four-layer active phase structures to 38% and 22% respectively. Based on the data in Fig. 6(a), the average stacking layer number ($\overline{N}$) was also calculated and summarized in Table 2. The results manifest the above discussions, that is, $\overline{N}$ of MoS_2 slabs on the sulfided catalysts increase in the order: AlB-0 (1.52) < AlB-2.0 (2.27) < AlB-2.0(MW) (2.72). The rise in the average slab numbers of active phase crystallites could increase the edge/rim ratio, providing more number of the desulfurization activity sites, and leading to efficient growth of HDS/HYDO selectivity [34].

From Fig. 6(b), modification has little effect on the average cluster length compared to that on the stacking

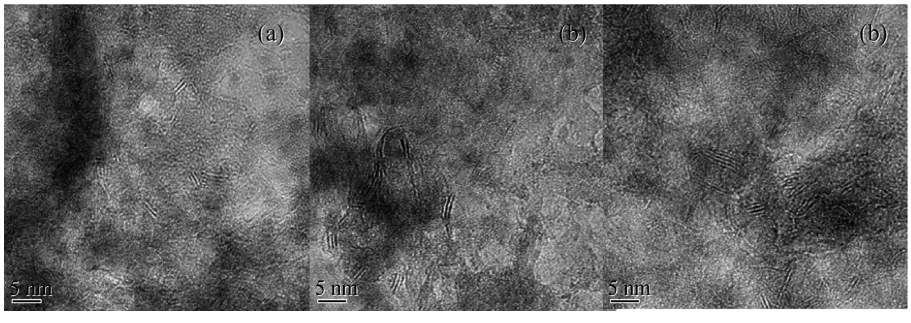

Fig. 5 HRTEM images of the sulfide catalysts: (a) AlB-0; (b) AlB-2.0; (c) AlB-2.0(MW).

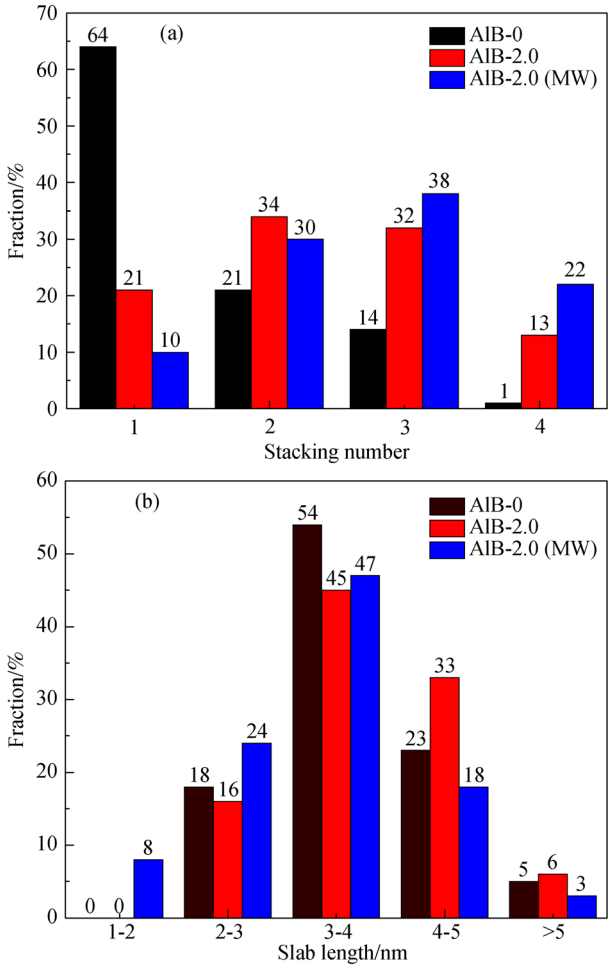

Fig. 6 (a) Distributions of the stacking number and (b) slab lengths of the sulfide catalysts.

numbers. It is clear that the average cluster length increases in the order AlB-2.0(MW) < AlB-0 < AlB-2.0, which means that microwave heating displays a significantly reduced cluster length. Although the cluster length has a significant influence on the number of edge and rim sites, shorter cluster length contributes to the higher distribution

Table 2 HRTEM analysis results of the sulfided catalysts

Catalyst	$\overline{L}$ /nm	$\overline{N}$	D_{Mo}
AlB-0	3.65	1.52	0.31
AlB-2.0	3.79	2.37	0.30
AlB-2.0(MW)	3.34	2.72	0.32

of the active components on the support [40]. More importantly, since the microwave-prepared catalyst has much higher stacking layers, the catalyst has the obvious advantage of an increased edge/rim ratio (as showed in Fig. 7). It would increase the amount of desulfurization activity sites and improve the desulfurization performance.

3.5 XPS characterization

The XPS characterization measurements were carried out, and the sulfurization degree of Mo species and the Co-Mo-S phase ratio for the three sulfided catalysts are summarized in Table 3. The Mo 3*d* XPS experimental spectra and their deconvolution results are shown in Fig. 8. According to the reported literatures [25,41], Mo 3*d* spectra can be fitted into the following species: the doublet at binding energies (BE) of 229.0 ± 0.1 and 232.1 ± 0.1 eV is originated to Mo $3d_{5/2}$ and Mo $3d_{3/2}$ of MoS_2 (Mo^{4+}); the BE of Mo $3d_{5/2}$ and Mo $3d_{3/2}$ of MoO_xS_y (Mo^{5+}) are 230.5 ± 0.1 and 233.7 ± 0.1 eV, respectively; the doublet at BE of 233.1 ± 0.1 and 236.0 ± 0.1 eV is attributed to Mo $3d_{5/2}$ and Mo $3d_{3/2}$ of MoO_3 (Mo^{6+}). Besides, the peak presented at 226.1 eV is assigned to S 2*s* level of sulfur. The larger area of peaks related to MoS_2 indicates higher sulfurization.

Mo sulfurization degree ($Mo_{sulfurization}/Mo_{total}$) directly affects the HDS performance of the catalyst, which can be defined as $Mo^{4+}/(Mo^{4+}+Mo^{5+}+Mo^{6+})$. From XPS analysis, Mo sulfurization degree increases in the following order: AlB-0 < AlB-2.0 < AlB-2.0(MW). The increased content of Mo^{4+} can be attributed to the weakened MSI and β-$CoMoO_4$ formation, which favors the sulfuridation of the Mo species to form Co-Mo-S II. It is obvious that the

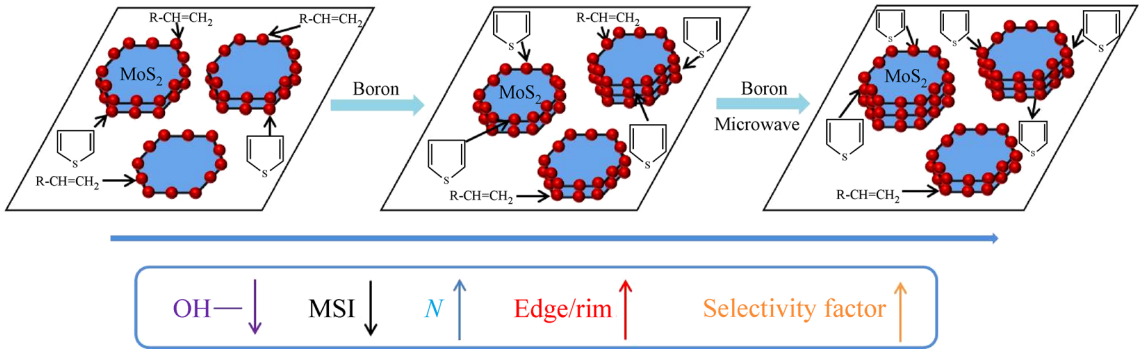

Fig. 7 Schematic illustration of boron influence on MoS_2 active phase morphology.

Table 3 Co and Mo species distribution at the surface of the sulfided catalysts

Catalysts	Mo distribution/%			Co distribution/%		
	Mo^{4+}	Mo^{5+}	Mo^{6+}	CoMoS	Co^{2+}	Co_9S_8
AlB-0	47.25	7.87	44.88	25.80	70.04	4.16
AlB-2.0	58.57	7.27	34.16	34.64	60.24	5.12
AlB-2.0(MW)	64.34	6.23	29.43	43.68	49.81	6.51

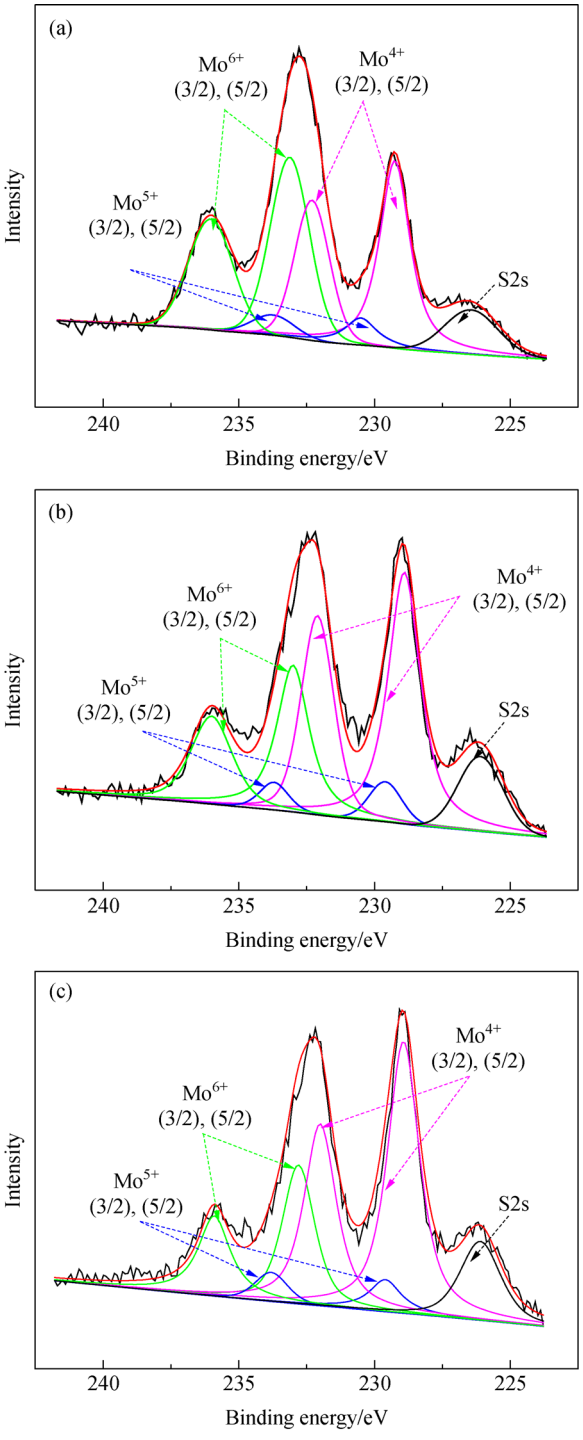

Fig. 8 Mo3*d* XPS spectra of the sulfided catalysts: (a) AlB-0; (b) AlB-2.0; (c) AlB-2.0(MW).

catalyst prepared by microwave heating further improve the effect. This result is evidenced by the H_2-TPR and HRTEM results.

The Co $2p_{3/2}$ XPS experimental spectra and their deconvolution results are shown in Fig. 9. According to the reported literature [40,42], the Co $2p_{3/2}$ spectra can be fitted into the following species: the peaks at BE of 779.2 ± 0.1, 781.6 ± 0.1 and 778.6 ± 0.1 eV are assigned to Co-Mo-S phase, Co^{2+} species (CoO_x and $CoAl_2O_4$) and Co_9S_8 phase, respectively. The proportion of Co-Mo-S phases over the prepared catalysts increase in the same order of Mo sulfidation degree. The increased content of MoS_2 induced by weak MSI will cause more interactions between Co and Mo species, which is more conductive to the formation of Co-Mo-S active phases [40].

3.6 HDS performance of the prepared catalysts

The effects of reaction temperatures on the HDS performance of FCC gasoline over AlB-0, AlB-2.0 and AlB-2.0(MW) catalysts were studied and summarized in Table 4. The results indicate that AlB-2.0 catalyst shows a higher HDS efficiency than that of AlB-0, e.g., the HDS ratio increased by 6%–16%, and the elevation degree at low temperature is higher than that at high temperatures. Drying and calcining of the catalysts by microwave heating can significantly improve the HDS activities. The evaluation results can be reflected from the H_2-TPR analysis. Meanwhile, the incorporation of microwave also increases the number of octahedral hexacoordinated Mo species, leading to a larger number of the Co-Mo-S II active phases, and thus improves desulfurization activity.

It can be seen from Table 5 that the selectivity index of AlB-2.0(MW) is significantly improved compared to that of AlB-2.0. HRTEM statistical results indicate that microwave heating highly increases the MoS_2 stacking number over the surface of γ-Al_2O_3, from 1.52 to 2.72. However, the cluster length decreases only from 3.65 to 3.34 nm. Because of that, the edge sites are highly increased than the corner sites, i.e., the edge/corner ratio of the catalyst prepared by microwave is highly increased. It has been well accepted that the edge sites are responsible for HDS reaction, while the corner sites can catalyze hydrogenation reactions. The above suggests that the higher edge/corner ratio can be achieved by microwave-assisted preparation, hence increasing the number of the desulfurization activity sites, and reducing the hydrogenation activity sites.

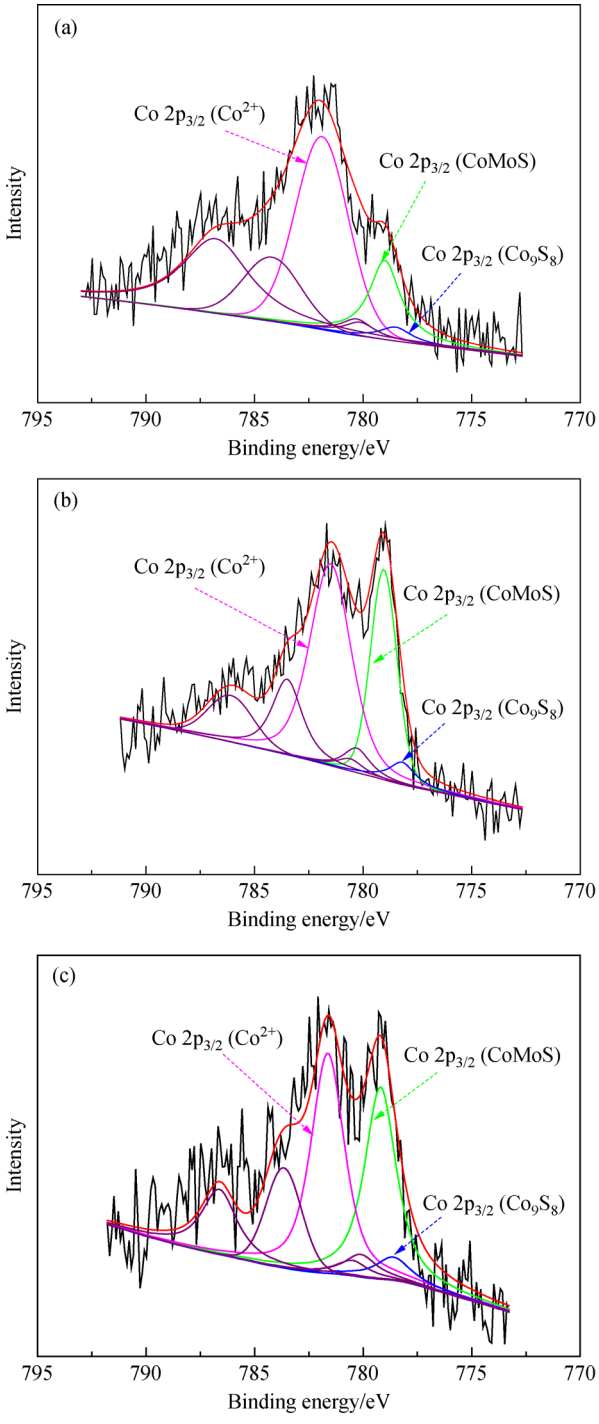

Fig. 9 Co $2p_{3/2}$ XPS spectra of the sulfided catalysts: (a) AlB-0; (b) AlB-2.0; (c) AlB-2.0(MW).

Table 4 HDS rate of boron modified catalyst at different temperatures

Sample	220 °C	240 °C	260 °C
AlB-0	51.84	79.41	87.31
AlB-2.0	67.75	90.10	93.43
AlB-2.0(MW)	74.75	96.37	97.82

Table 5 HDS, HYDO and HDS/HYDO of boron modified catalyst at 260 °C

Sample	HDS rate/%	HYDO rate/%	HDS/HYDO
AlB-0	87.31	53.30	2.71
AlB-2.0	93.43	52.26	3.68
AlB-2.0(MW)	97.82	50.52	5.44

4 Conclusions

Boron was used as an additive to modify CoMo/γ-Al_2O_3 catalysts. The physicochemical properties and catalytic properties of the modified catalysts were analyzed by BET, SEM, py-FTIR, H_2-TPR, HRTEM, XPS and the hydrodesulfurization evaluation. Results show that the addition of boron could weaken the interaction between the active component and the support, and then the number of stacking layers of the active phases increased, improving the formation of more highly active Co-Mo-S II active phases. It should also be noticed that microwave treatment can efficiently increase the surface area and pore size by rapid dehydroxylation, leading to the formation of more clean and open pore structures. The HDS evaluation results indicated that boron modification not only improved the desulfurization activity, but also retained more olefin components, i.e., increasing the selectivity coefficient of the catalyst.

HDS results from the catalyst prepared by adopting microwave heating method suggest that microwave heating benefits to the weaker interaction between the active component and the support and can improve the distribution of the active components. The microwave-assisted catalyst exhibits a higher desulfurization rate, maintained a lower olefin saturation rate, and hence results in a greater selectivity factor.

Acknowledgements This work was supported by the National Natural Science Foundation of China (Grant No. 21476258).

References

1. Song C S, Ma X L. Ultra-clean diesel fuels by deep desulfurization and deep dearomatization of middle distillates. Journal of Biomechanics, 2006, 43(3): 579–582
2. Singh R, Kunzru D, Sivakumar S. Monodispersed ultrasmall NiMo metal oxide nanoclusters as hydrodesulfurization catalyst. Applied Catalysis B: Environmental, 2016, 185: 163–173
3. Song C S. An overview of new approaches to deep desulfurization for ultra-clean gasoline, diesel fuel and jet fuel. Catalysis Today, 2003, 86(1): 211–263
4. Duan A J, Li T S, Zhao Z, Liu B J, Zhou X F, Jiang G Y, Liu J, Wei Y C, Pan H F. Synthesis of hierarchically porous L-KIT-6 silica-alumina material and the super catalytic performances for hydrodesulfurization of benzothiophene. Applied Catalysis B: Environmental, 2015, 165: 763–773

5. Li M F, Li H F, Jiang F, Chu Y, Nie H. The relation between morphology of (Co)MoS_2 phases and selective hydrodesulfurization for CoMo catalysts. Catalysis Today, 2010, 149(1-2): 35–39
6. Topsøie H, Candia R, Topsøe N Y, Clausen B, Topsøe H. On the state of the Co-Mo-S model. Bulletin des Sociétés Chimiques Belges, 1984, 93(8-9): 783–806
7. Topsøie H, Clausen B S, Topsøe N Y, Pedersen E. Recent basic research in hydrodesulfurization catalysis. Industrial & Engineering Chemistry Fundamentals, 1986, 25(1): 25–36
8. Topsøe H, Clausen B S, Massoth F E. Hydrotreating Catalysis. Berlin: Springer, 1996, 116–118
9. Chen W B, Maugé F, van Gestel J, Nie H, Li D D, Long X Y. Effect of modification of the alumina acidity on the properties of supported Mo and CoMo sulfide catalysts. Journal of Catalysis, 2013, 304: 47–62
10. Vatutina Y V, Klimov O V, Nadeina K A, Danilova I G, Gerasimov E Y, Prosvirin I P, Noskov A S. Influence of boron addition to alumina support by kneading on morphology and activity of HDS catalysts. Applied Catalysis B: Environmental, 2016, 199: 23–32
11. Bautista F M, Campelo J M, Garcia A, Luna D, Marinas J M, Moreno M C, Romero A A, Navio J A, Macias M. Structural and textural characterization of $AlPO_4$-B_2O_3 and Al_2O_3-B_2O_3(5–30 wt-% B_2O_3) systems obtained by boric acid impregnation. Journal of Catalysis, 1998, 173(2): 333–344
12. Dhar G M, Srinivas B N, Rana M S, Kumar M, Maity S K. Mixed oxide supported hydrodesulfurization catalysts—a review. Catalysis Today, 2003, 86(1): 45–60
13. de Farias A M D, Esteves A M L, Ziarelli F, Caldarelli S, Fraga M A, Appel L G. Boria modified alumina probed by methanol dehydration and IR spectroscopy. Applied Surface Science, 2004, 227(1): 132–138
14. Torres-Mancera P, Ramírez J, Cuevas R, Gutiérrez-Alejandre A, Murrieta F, Luna R. Hydrodesulfurization of 4,6-DMDBT on NiMo and CoMo catalysts supported on B_2O_3-Al_2O_3. Catalysis Today, 2005, 107-108: 551–558
15. Ding L H, Zhang Z S, Zheng Y, Ring Z, Chen J W. Effect of fluorine and boron modification on the HDS, HDN and HDA activity of hydrotreating catalysts. Applied Catalysis A, General, 2006, 301(2): 241–250
16. Usman, Kubota T, Hiromitsu I, Okamoto Y. Effect of boron addition on the surface structure of Co-Mo/Al_2O_3 catalysts. Journal of Catalysis, 2007, 247(1): 78–85
17. Palcheva R, Kaluza L, Spojakina A, Jiratova K, Tyuliev G. NiMo/γ-Al_2O_3 catalysts from Ni heteropolyoxomolybdate and effect of alumina modification by B, Co, or Ni. Chinese Journal of Catalysis, 2012, 33(6): 952–961
18. Peil K P, Galya L G, Marcelin G. Acid and catalytic properties of nonstoichiometric aluminum borates. Journal of Catalysis, 1989, 115(2): 441–451
19. Pérez-Martínez D J, Eloy P, Gaigneaux E M A, Giraldo S, Centeno A. Study of the selectivity in FCC naphtha hydrotreating by modifying the acid–base balance of CoMo/γ-Al_2O_3 catalysts. Applied Catalysis A, General, 2010, 390(1): 59–70
20. Houalla M, Delmon B. Joint use of xps and diffuse reflectance spectroscopy for the study of cobalt oxide supported on boron modified alumina. Applied Catalysis, 1981, 1(5): 285–289
21. Morishige H, Akai Y. Effect of boron addition on the state and dispersion of Mo supported on alumina. Bulletin des Sociétés Chimiques Belges, 1995, 104(4-5): 253–257
22. Lewandowski M, Sarbak Z. Acid-base properties and the hydrofining activity of NiMo catalysts incorporated on alumina modified with F^- and Cl^-. Applied Catalysis A, General, 1997, 156(2): 181–192
23. Lewandowski M, Sarbak Z. The effect of boron addition on hydrodesulfurization and hydrodenitrogenation activity of NiMo/Al_2O_3 catalysts. Fuel, 2000, 79(5): 487–495
24. Rashidi F, Sasaki T, Rashidi A M, Kharat A N, Jozani K J. Ultradeep hydrodesulfurization of diesel fuels using highly efficient nanoalumina-supported catalysts: impact of support, phosphorus, and/or boron on the structure and catalytic activity. Journal of Catalysis, 2013, 299: 321–335
25. Klimov O V, Nadeina K A, Vatutina Y V, Stolyarova E A, Danilova I G, Gerasimov E Y, Prosvirin I P, Noskov A S. CoMo/Al_2O_3 hydrotreating catalysts of diesel fuel with improved hydrodenitrogenation activity. Catalysis Today, 2018, 307: 73–83
26. Shang H, Zhang H C, Du W, Liu Z C. Development of microwave assisted oxidative desulfurization of petroleum oils: a review. Journal of Industrial and Engineering Chemistry, 2013, 19(5): 1426–1432
27. Wang H, Wu Y, Liu Z W, He L, Yao Z Y, Zhao W Y. Deposition of WO_3 on Al_2O_3 via a microwave hydrothermal method to prepare highly dispersed W/Al_2O_3 hydrodesulfurization catalyst. Fuel, 2014, 136: 185–193
28. Wang H, Yao Z Y, Zhan X C, Wu Y, Li M. Preparation of highly dispersed W/ZrO_2-Al_2O_3 hydrodesulfurization catalysts at high WO_3 loading via a microwave hydrothermal method. Fuel, 2015, 158: 918–926
29. Wang H, Liu Z W, Wu Y, Yao Z Y, Zhao W Y, Duan W Z, Guo K. Preparation of highly dispersed W/Al_2O_3 hydrodesulfurization catalysts via a microwave hydrothermal method: effect of oxalic acid. Arabian Journal of Chemistry, 2016, 9(1): 18–24
30. Liu X F, Zhang L, Shi Y H, Nie H, Long X Y. Preparation of NiW/Al_2O_3 hydrodesulfurization catalyst by ultrasound-microwave treatment. Chinese Journal of Catalysis, 2004, 25(9): 748–752
31. Liu B J, Zha X J, Meng Q M, Hou H J, Gao S S, Zhang J X, Sheng S S, Yang W S. Preparation of NiW/TiO_2-Al_2O_3 hydrodesulfurization catalyst with microwave technique. Chinese Journal of Catalysis, 2005, 26(6): 458–462
32. Meredith R. Engineers Handbook of Industrial Microwave Heating. London: Institute of Electrical Engineers, 1998, 19–20
33. Badoga S, Sharma R V, Dalai A K, Adjaye J. Synthesis and characterization of mesoporous aluminas with different pore sizes: application in NiMo supported catalyst for hydrotreating of heavy gas oil. Applied Catalysis A, General, 2015, 489: 86–97
34. Zhang C, Liu X Y, Liu T F, Jiang Z X, Li C. Optimizing both the CoMo/Al_2O_3 catalyst and the technology for selectivity enhancement in the hydrodesulfurization of FCC gasoline. Applied Catalysis A, General, 2019, 575: 187–197
35. Zhou W W, Yang L, Liu L, Chen Z P, Zhou A N, Zhang Y T, He X F, Shi F X, Zhao Z G. Synthesis of novel NiMo catalysts supported on highly ordered TiO_2-Al_2O_3 composites and their superior catalytic performance for 4,6-dimethyldibenzothiophene hydrode-

sulfurization. Applied Catalysis B: Environmental, 2020, 268: 118428

36. Shan S F, Yuan P, Han W, Shi G, Bao X J. Supported NiW catalysts with tunable size and morphology of active phases for highly selective hydrodesulfurization of fluid catalytic cracking naphtha. Journal of Catalysis, 2015, 330: 288–301
37. Wang X, Zhao Z, Zheng P, Chen Z, Duan A, Xu C, Jiao J, Zhang H, Cao Z, Ge B. Synthesis of NiMo catalysts supported on mesoporous Al_2O_3 with different crystal forms and superior catalytic performance for the hydrodesulfurization of dibenzothiophene and 4,6-dimethyldibenzothiophene. Journal of Catalysis, 2016, 344: 680–691
38. Brito J L, Barbosa A L. Effect of phase composition of the oxidic precursor on the HDS activity of the sulfided molybdates of Fe(II), Co(II), and Ni(II). Journal of Catalysis, 1997, 171(2): 467–475
39. Lizama L, Klimova T. Highly active deep HDS catalysts prepared using Mo and W heteropolyacids supported on SBA-15. Applied Catalysis B: Environmental, 2008, 82(3-4): 139–150
40. Zhang C, Brorson M, Li P, Liu X, Liu T, Jiang Z, Li C. $CoMo/Al_2O_3$ catalysts prepared by tailoring the surface properties of alumina for highly selective hydrodesulfurization of FCC gasoline. Applied Catalysis A, General, 2019, 570: 84–95
41. Xia B T, Cao L Y, Luo K W, Zhao L, Wang X Q, Gao J S, Xu C M. Effects of the active phase of $CoMo/\gamma\text{-}Al_2O_3$ catalysts modified using cerium and phosphorus on the HDS performance for FCC gasoline. Energy & Fuels, 2019, 33(5): 4462–4473
42. Huang T T, Xu J D, Fan Y. Effects of concentration and microstructure of active phases on the selective hydrodesulfurization performance of sulfided $CoMo/Al_2O_3$ catalysts. Applied Catalysis B: Environmental, 2018, 220: 42–56